Environmental Science & Technology

Article

pubs.acs.org/est

Efficient Filtration of Effluent Organic Matter by Polycation-Clay Composite Sorbents: Effect of Polycation Configuration on Pharmaceutical Removal

Itamar A. Shabtai and Yael G. Mishael*

Dept. Soil and Water Sci., The Robert H. Smith Faculty of Agriculture, Food and Environment, Hebrew University of Jerusalem, Rehovot, Israel

Supporting Information

ABSTRACT: Hybrid polycation-clay composites, based on methylated poly vinylpyridinium, were optimized as sorbents for secondary effluent organic matter (EfOM) including emerging micropollutants. Composite structure was tuned by solution ionic strength and characterized by zeta potential, FTIR, X-ray diffraction, and thermal gravimetric analyses. An increase in ionic strength induced a transition from a train to a loops and tails configuration, accompanied by greater polycation adsorption. Composite charge reversal (zeta potential −18 to 45 mV) increased the adsorption of EfOM and humic acid (HA), moderately and sharply, respectively, suggesting electrostatic and also nonspecific interactions with EfOM. Filtration of EfOM by columns of positively charged composites was superior to that of granular activated carbon (GAC). The overall removal of EfOM was most efficient by the composite with a train configuration. Whereas a composite with a loops and tails configuration was beneficial for the removal of the anionic micropollutants diclofenac, gemfibrozil and ibuprofen from EfOM. These new findings suggest that the loops and tails may offer unique binding sites for small micropollutants which are overseen by the bulk EfOM. Furthermore, they may explain our previous observations that in the presence of dissolved organic matter, micropollutant filtration by GAC columns was reduced, while their filtration by composite columns remained high.

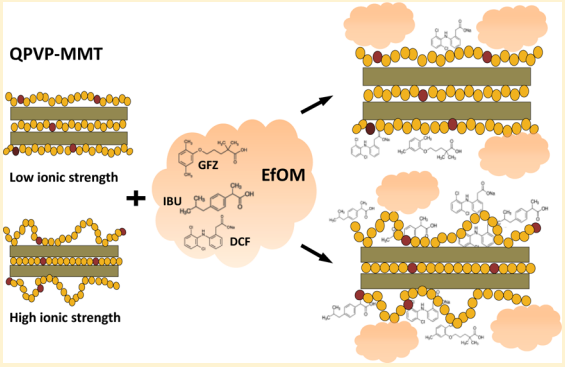

INTRODUCTION

As the world faces water supply challenges, water reuse, including highly treated wastewater effluent for irrigation and even for potable use, is increasingly drawing attention.[1] Secondary treated effluent contains effluent organic matter (EfOM) which mainly consists of biological treatment derived soluble microbial products, refractory humic substances derived from drinking water, inorganic ions and trace levels of organic micropollutants including pharmaceuticals.[2−6] Reuse of secondary effluent for irrigation usually necessitates tertiary treatment[7] such as soil aquifer treatment (SAT). The SAT process includes recharging secondary effluent through a sandy soil aquifer, where it is retained, and then pumped for reuse.[8] SAT has been proven to efficiently remove EfOM, microorganisms, suspended particles, and inorganic and organic micropollutants, through biological oxidation, filtration, and adsorption to soil minerals.[9]

Since the late 1980s a SAT operation has been carried out at the Dan Region Wastewater Reclamation Plant (Shafdan) in Israel, generating tertiary treated wastewater for unrestricted irrigation.[7,9,10] However, several geochemical changes have been taking place ensuing decades of SAT operation, leading to operational challenges. Accumulation of organic matter in the soil[9] has been associated with hydrophobicity and water repellency, which in turn, has reduced recharge rates.[10,11] In addition, EfOM-associated reductive dissolution of manganese, and its subsequent precipitation to Mn-oxides, is accompanied by pipe blockage and other infrastructural problems.[12]

These issues have prompted pretreatment of secondary effluent to reduce EfOM prior to SAT. Ultrafiltration, ozonation, coagulation and UV disinfection have been suggested. However, these treatments can be energy and chemical intensive, as EfOM exerts higher coagulant and oxidant demands[4,13] and impedes filtration processes due to membrane biofouling.[14−16] Oxidation treatments also promote a wide range of disinfection by products.[17,18] Adsorption to granular activated carbon (GAC) has been considered, in combination with other processes, yielding varying degrees of success.[4,19−22]

In recent years, there has been much interest in modified clays as novel, low cost sorbents, enabling efficient removal of organic micropollutants.[23−25] We have developed and employed polycation-montmorillonite clay (MMT) composites as sorbents for filtration of various organic micropollutants, in

Received: May 1, 2016
Accepted: July 10, 2016
Published: July 10, 2016

DOI: 10.1021/acs.est.6b02167
Environ. Sci. Technol. 2016, 50, 8246−8254

the presence of dissolved organic matter (DOM) or humic acid (HA).[26−28] The designed composites were based on poly-4-vinylpyridine-*co*-styrene (PVP), protonated PVP (HPVP) and methylated PVP (QPVP), for the removal of pyrene,[27] atrazine[26] and diclofenac,[28] respectively. In all cases, the filtration of the micropollutants by columns of the designed composite was more efficient than by GAC columns. More importantly, in the presence of DOM (for atrazine) or HA (for pyrene and diclofenac) micropollutant filtration by the GAC columns was reduced, as reported by many studies,[29,30] while the removal of the micropollutants by the composite columns was not compromised and remained high.

This high removal of micropollutants in the presence of DOM by the PVP composites was not fully understood but three main mechanisms were suggested: coadsorption (as concluded in the case of pyrene[27]), competition and/or independently.[28] To unveil which mechanisms are involved it is necessary to 1. Investigate pollutant-DOM interactions 2. Explore DOM removal by the composites and, most challenging 3. To distinguish between the adsorption sites of the DOM and the micropollutants. Anionic pharmaceuticals (at environmentally relevant pH) were selected to minimize pollutant-DOM interactions, excluding coadsorption. Our previous study on diclofenac (DCF) removal by QPVP-MMT composites suggested that at high polycation loadings in which the polycation adopts a loops and tails configuration, DCF may adsorb to unique sites on the composite, implying that independent adsorption may occur.[28]

In the current study we explored the filtration of EfOM from the Shafdan by GAC and by QPVP-MMT composites and aimed to elucidate the role of QPVP configuration (at the adsorbed state) in the removal of EfOM, and anionic pharmaceuticals commonly detected in the effluent: diclofenac (DCF), ibuprofen (IBP) and gemfibrozil (GFZ). QPVP loading and configuration on the clay were tuned by polycation solution ionic strength (*IS*) and the effect of both properties on removal efficiency was tested. The effect of solution *IS* on the interactions between oppositely charged colloids (polycations and clay minerals) has been investigated experimentally and modeled.[31−34] However, the consequent effect of polycation loading and configuration on composite functionality, that is, binding abilities, has not been widely explored and therefore is addressed here.

MATERIALS AND METHODS

Materials. Wyoming Na-montmorillonite SWy-2 (MMT) was obtained from the Source Clays Repository of the Clay Mineral Society (Columbia, MO). Poly(4-vinylpyridine-*co*-styrene) (PVP; M_W = 1200−1500 kDa; 9/1 pyridine/styrene), dimethylformamide, methyl iodide, humic acid sodium salt technical grade (HA), diclofenac sodium salt (pK_a 4.15), gemfibrozil (pK_a 4.42) and ibuprofen (pK_a 4.34) and all other reagents were purchased from Sigma-Aldrich. Dialysis bags with a cutoff of 1000 Da were used (Spectra/Por 6, Spectrumlabs). Granular activated carbon (GAC) was NORIT GAC 1240. A peat bog based GAC, 8−20 mesh, was purchased from Sigma-Aldrich (only used in the experiment outlined in Figure 7, denoted GAC 2). Quartz sand (grain size 0.8−1.5 mm) was purchased from Shoshani and Weinstein (Israel). Sandy soil (<2 mm) was sampled from the vicinity of SAT infiltration sites (not subjected to SAT in the past) and denoted Shafdan soil. The sandy media were washed in deionized water until supernatant was free of dissolved carbon and UV absorbance and dried at 105 °C. Stock solutions of HA (50 mg/L) were prepared as described,[35] filtered through a 0.45 μm filter paper, diluted with filtered tap water to the required concentration, and used immediately (pH 7.8). Secondary effluent (prior to SAT) from the Shafdan (Supporting Information (SI) S1 for effluent properties) was collected, immediately refrigerated (2 °C) and used within 24 h.

Methods. *Composite Preparation.* Preparation of methylated PVP (QPVP) and polycation-clay composites was carried out as described.[26,28] Briefly, MMT clay suspension (1.67 g/L, 0.5 mL) was added to QPVP solutions (0.05−2 g/L, 1 mL) in Eppendorf vials (1.5 mL). In addition, QPVP (2 g/L) adsorption on MMT (1.67 g/L) was determined as a function of polycation solution *IS* (0−4 M NaCl). The clay-polycation suspensions were agitated for 2 h (equilibrium was reached within 1 h) using a shaker, centrifuged (10 000*g*; 15 min), and supernatants were separated from the settled composites which were washed with deionized water (1.5 mL) and centrifuged again.

The absorbance of the supernatants was measured using UV−Vis spectrophotometry (Thermo Scientific, Evolution 300, Waltham, MA) at an excitation wavelength of 256 nm. A standard calibration curve was fitted and the amount of polycation adsorbed was calculated accordingly. Composites prepared for column experiments were prepared in a 20 L glass carboy and gently mixed with a magnetic stirrer for 2 h. QPVP-MMT composites prepared from polycation solution with *IS* of 0 M, 0.01 and 1 M, are denoted QPVP 0 M-, QPVP 0.01 M-, and QPVP 1 M-MMT, respectively.

Composite Characterization. FTIR Measurements. The spectra were obtained by pellets (100 mg) from freeze-dried QPVP solutions (3 g/L, 1 mg) and QPVP-MMT composites (2 mg) prepared at different *IS* mixed with KBr and recorded at room temperature in the range of 500−4000 cm^{-1} using an FTIR spectrometer (Nicolet Magna-IR-550, Madison WI).

X-ray Diffraction (XRD) Measurements. The basal (d 001) spacings of QPVP-MMT composites prepared at different *IS* were measured by XRD. Composite suspensions (1−2 mL; 0.1%) were placed on a glass slide and left to sediment (oriented sample) for 1 day. The basal spacing was measured using an X-ray diffractometer (Philips PW1830/3710/3020) with Cu KR radiation, λ = 1.526 Å.

Thermal Measurements. Thermal gravimetric analysis (TGA) of freeze-dried, air equilibrated QPVP and QPVP-MMT composites prepared at different *IS* were carried out on a Q500 Thermogravimetric Analyzer (TA Instruments Inc.). Heating rate was 10 °C/min using the high resolution-dynamic program (sensitivity 3, resolution 2); temperature ranged from 30 to 900 °C; air flow rate was 60 mL/min.

Zeta Potential Measurements. Zeta potentials of 0.1% (w/w) suspensions of GAC and QPVP-MMT composites (0.1−2.8 mmol QPVP/g clay) were measured using a Zetasizer Nanosystem (Malvern Instruments, Southborough, MA).

Exchangeable Anion Capacity. Upon QPVP adsorption to the clay the counter-anions (I^- and Cl^-) of the monomers which are in direct interaction with the clay are released. The exchangeable anion capacity (QPVP monomers not in direct interaction with the clay) of QPVP composites was determined by displacement of the counteranions with bromide. QPVP 0 M-, QPVP 0.01 M-, and QPVP 1 M-MMT (22 mg) were dialyzed (Spectra/Por 6, molecular weight cutoff 1000 da) against several changes of deionized water to remove excess electrolytes and low-weight polycation fractions (monitored by

DOI: 10.1021/acs.est.6b02167
Environ. Sci. Technol. 2016, 50, 8246−8254

EC (electrical conductivity) and UV absorbance at 256 nm, respectively). Since QPVP 0.01 M-MMT and QPVP 1 M-MMT contain chloride as well as iodide, they were first saturated with iodide by repeated dialysis against potassium iodide (200 mL, 1 mM) and then against deionized water, to remove excess iodide and electrolyte. Then, KBr (200 mL, 5 mM) was added to the solution surrounding the dialysis bags containing the composites and stirred for 24 h. The concentration of iodide in the dialysate was determined by UV absorbance at 226 nm. The KBr solution was replaced repeatedly to ensure complete exchange of iodide. A calibration curve was prepared with potassium iodide and the exchangeable anion capacity was calculated accordingly.

Analysis of EfOM and HA. Samples of EfOM and HA were filtered through a 0.45 μm Acrodisc syringe filter prior to measurement.

Zeta Potential Measurements. Zeta potentials of Shafdan effluent (12.2 mg/L dissolved organic carbon (DOC)) and HA (3 mg/L (DOC)) solutions were measured as described above.

UV−Vis Spectrophotometry. UV absorbance at a wavelength of 254 nm (UV_{254}) was measured (Thermo Scientific, Evolution 300, Waltham, MA).

Dissolved Organic Carbon (DOC) Measurements. DOC (mg/L) was measured at the Nesin laboratory of Mekorot, National Water Carrier, following the Standard Methods.[36]

Comparison of UV−Vis and DOC Measurements. Shafdan secondary effluent was passed through QPVP-MMT, Shafdan soil and GAC columns (see details below). The DOC content and UV_{254} of the eluent were determined (as described above) at timed intervals, and their values plotted against each other for the GAC and composite columns separately. Since no significant difference between sorbents was observed, a statistically significant ($P < 0.0001$) regression was obtained for the whole data set (SI Figure S2), as reported elsewhere (Goren et al., 2008). This indicated that UV−vis spectrophotometry may be used to compare the removal efficiency of the different sorbents.

Removal of EfOM and Humic Acid by QPVP-MMT Composites and GAC. EfOM and HA Adsorption to QPVP-MMT Composites. EfOM (12.2 mg/L DOC) or HA (3 mg/L DOC) were added to centrifuge tubes containing QPVP-MMT composites (0−1.1 mmol QPVP/g clay). In both cases, the ratio of added dissolved organics to clay was 18 mg DOC/g clay. Control samples (i.e., HA or EfOM without sorbent) were included. The tubes were agitated for 24 h, supernatants were separated by centrifugation (10000 g; 15 min) and their UV_{254} was measured. Amount of EfOM or HA adsorbed (% removal) was calculated accordingly.

Filtration of EfOM and HA by QPVP-MMT and GAC Columns. Glass columns (20 cm length, 1 cm diameter, 6 mL pore volume) were filled with 20 g of quartz sand and 0.2 g sorbent (Low QPVP-MMT and QPVP 0 M-, 0.01 M- and 1 M-MMT, or GAC) to achieve a weight ratio of 1:100 (w/w). The sorbents were mixed with excess quartz sand to enable a high flow rate through the column. These composite columns were washed by passing tap water, and polycation concentration in the leachate was monitored and quantified by UV−vis, as described above. Cumulative polycation desorption from each composite was ∼5% of initial polycation content. No polycation was detected in the water after 18 pore volumes for QPVP 0 M- and 0.01 M-MMT and after 130 pore volumes for QPVP 1 M-MMT (SI Figure S3).

Filtration of HA (3 mg/L DOC) and Shafdan EfOM (12.2 mg/L DOC) by the columns was studied (150−200 pore volumes). Experiments were carried out in duplicates at 25 °C, at a flow rate of 2 mL/min, obtaining a filter velocity of 1.5 m/h.

A filtration experiment at higher composite/sand ratio (1:20 (w/w)) testing the most efficient composite was conducted. Glass columns (20 cm length, 1.5 cm diameter, 30 mL pore volume) were filled with either Shafdan soil (74 g), QPVP 0 M-MMT or GAC (3.5 g) mixed with 70.5 g of quartz sand. Shafdan secondary effluent was passed through each of the filters at a flow rate of 3.6 mL/min, obtaining a filter velocity of 1.3 m/h. The eluents and stock solutions were collected in timed intervals and analyzed for EfOM concentration by UV−vis spectrophotometry. UV_{254} and DOC of Shafdan effluent and HA stock solution remained constant in the time frame of the filtration experiments.

Removal of Anionic Micropollutants by QPVP Composites. Micropollutant Analysis. Micropollutant concentration in the supernatants was measured by an Agilent 1200 series HPLC instrument equipped with a G1315D diode-array detector and a G1321A fluorescence detector. HPLC column was Phenomenex Luna C18(2) (5 μm). DCF was measured with the diode-array detector (λ = 276 nm) and IBU and GFZ were measured by fluorescence (λ_{ex} = 210 λ_{em} = 300 nm and λ_{ex} = 220 λ_{em} = 300 nm, respectively). Measurements were carried out isocratically at 30 °C. The mobile phase was acetonitrile and acidified double distilled water (0.1% formic acid) (80/20 for DCF and GFZ and 90/10 for IBU). The flow rate was 1 mL/min for DCF and GFZ and 1.2 mL/min for IBU. LOQ was 0.05, 0.025, and 0.05 mg/L for DCF, GFZ, and IBU, respectively. Initial micropollutant concentration in the Shafdan effluent (SI Table S1) was below the LOD of the above method.

Adsorption of Micropollutant to QPVP Composites. Stock solutions of DCF, GFZ, and IBU were prepared in methanol (30, 17, 15 mg/mL). Tap water or Shafdan effluent (pH 7.8) were spiked (0.1% v/v) with the above stock solutions yielding working solutions of DCF, GFZ, and IBU, (30 mg/L, 0.094 mM) (17 mg/L, 0.068 mM), (15 mg/L, 0.073 mM), respectively. These concentrations correspond to approximately 12 mg DOC/L, similar to the DOC concentration of EfOM in the Shafdan effluent. Micropollutant working solutions were added to 50 mL Teflon tubes containing QPVP 0 M-, QPVP 0.01 M- or QPVP 1 M-MMT composites (1.67 g/L) and agitated for 24 h. Supernatants were separated by centrifugation (10 000g; 15 min) and filtered with 0.45 μm PTFE syringe filters (AXIVA). Analyte loss in control samples (i.e., micro pollutant without composite) was negligible.

Anionic Micropollutant Interactions with EfOM. Shafdan effluent (50 mL) was added to dialysis bags (1000 Da cutoff) and immersed in tap water (150 mL) (to minimize excess dilution of electrolyte) which was spiked with DCF, GFZ or IBU to obtain a final concentration of 20, 11.3, and 10 mg/L, respectively, and agitated for 48 h. Micropollutant concentrations inside and outside of the dialysis bags were determined. Different micropollutant concentrations inside and outside the bags would suggest micropollutant-EfOM interactions. However, the concentration of DCF, GFZ, and IBU inside and outside of the dialysis bag did not differ significantly, indicating that interactions between negatively charged EfOM and micropollutants were negligible, as expected.

DOI: 10.1021/acs.est.6b02167
Environ. Sci. Technol. 2016, 50, 8246−8254

Control samples which included the micropollutants in the absence of effluent, verified that DCF, GFZ, or IBU concentrations inside and outside the dialysis bag were equal. Adsorption of the tested micropollutants to the dialysis bag was found to be negligible (<%5). Micropollutant concentration did not decrease upon incubation with Shafdan effluent (48 h). Additional control tubes containing Shafdan effluent (in the absence of micropollutants) indicated that approximately 50% of the EfOM diffused outside the dialysis bags as previously reported.[37,38] The low molecular weight fraction was not discarded in order to determine the interactions of the micropollutants with both EfOM size fractions.

RESULTS AND DISCUSSION

Effect of *IS* on QPVP Adsorption to Clay. Polycation configuration on a surface is strongly affected by its loading.[39] At a low polycation loading the polycation adopts a flat configuration of trains, whereas at high loadings an additional configuration of loops and tails is obtained. Recently we have reported the effect of QPVP loading, reached by increasing QPVP concentration, on polycation configuration.[28] However, the important effect of polycation solution *IS* on QPVP loading and consequently on its configuration has not been addressed. To study this effect QPVP adsorption from solutions with increasing *IS* (NaCl 0−4 M) was determined (Figure 1) and characterized (Figure 2).

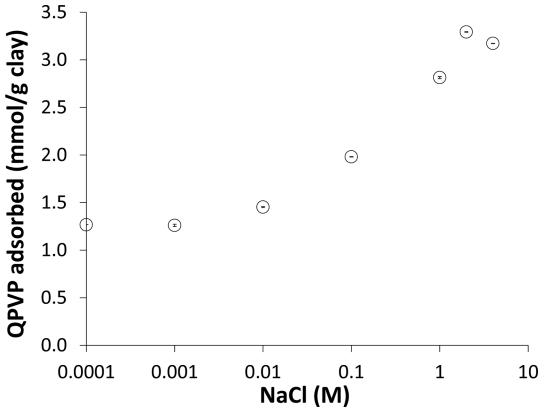

Figure 1. QPVP (2 g/L) adsorption on clay (1.67 g/L) as a function of solution NaCl concentration.

Polycation adsorption increased with an increase in *IS* while a decrease in polycation adsorption was observed for a very high *IS* (Figure 1). Similar trends were obtained both theoretically[32,34] and experimentally for several highly charged polycations, including poly(diallyldimethylammonium chloride),[33] poly(4-vinyl *N*-methylpyridinium iodide) (QPVP),[31,33,39] maleimide propyl trimethylammonium chloride on silica[40] and cationic polyacrylamides on montmorillonite clay.[41] At low salt concentrations, resulting in large Debye lengths, electrostatic repulsion between charged polycation segments limited polycation adsorption. Increasing *IS* screened segment−segment repulsion, thereby enabling greater polycation adsorption. A further increase in *IS* (4 M) screened more short-range interactions between polycation segments and the negatively charged surface, and therefore adsorption decreased. Maximum adsorption of QPVP was reached at 2 M NaCl (similar to its adsorption on silica).[31,39]

Composites prepared from polycation solutions of 0, 0.01, and 1 M NaCl were denoted QPVP 0 M-, QPVP 0.01 M- and QPVP 1 M-MMT (QPVP loadings were 0.13, 0.15, and 0.3 g QPVP/g clay, respectively). Above composites were further characterized by FTIR (Figure 2a), XRD (Figure 2b) and TGA (Figure 2c). The characteristic bands of PVP at 1555 and 1597 cm^{-1} are assigned to C═C and C═N stretching in the pyridyl ring, respectively (Figure 2a).[42−44] These bands disappeared upon methylation (QPVP sample) and three characteristic vibrations at 1519, 1575, and 1643 cm^{-1} appeared. The 1643 cm^{-1} band is indicative of formation of a quaternary amine group.[42,44] Once adsorbed, a red shift of the 1643 cm^{-1} band to 1663 cm^{-1} was measured for the QPVP 0 M-MMT composite, suggesting electrostatic interaction between QPVP and the clay surface.[28] For the QPVP 0.01 M- and QPVP 1 M-MMT composites only a shoulder is obtained at 1663 cm^{-1} while a dominant peak is observed at 1643 cm^{-1}, indicating that a large fraction of the pyridinium groups are not directly interacting with the clay. As *IS* increased to 0.01 M and to 1 M the ratio of clay-associated pyridinium/free pyridinium decreased. These results suggest that increased *IS* led to a QPVP configuration in which pyridinium groups extend into solution as loops and tails. Additional confirmation of QPVP configuration at the adsorbed state was provided by the anion exchange capacity of the composites, which was 0.38, 0.58, and 0.68 mmol/mmol QPVP monomers of QPVP 0 M-, QPVP 0.01 M-, and QPVP 1 M-MMT, respectively.

Consequently, QPVP 0 M- and QPVP 0.01 M-MMT were characterized as having similar loadings (0.13 and 0.15 g/g clay, respectively), but different polycation configurations.

A more extended configuration of QPVP at high *IS* was supported by XRD measurements (Figure 2b). As solution *IS* increased (0 to 0.01 and 1 M), *d*-spacing decreased from 1.51 to 1.3 nm. A decrease in the *d*-spacing upon an increase in QPVP loading has been reported and attributed to water exclusion upon increased polycation intercalation.[28]An additional diffraction at small angles (2θ) and general broadening of the 1.3 nm diffraction was obtained for the QPVP 1 M composite, indicating a more heterogeneous structure, including partial exfoliation and intercalation, respectively.

Finally, the suggested shift in QPVP configuration (at the adsorbed state) from a flat one to more extended one, upon an increase in *IS* was reinforced by TGA measurements (Figure 2c). Polycation intercalation with and without complete water exclusion for the QPVP 1 M-MMT and QPVP 0 M-MMT, respectively, is supported by the mass loss only for the latter composite at ∼105 °C, ascribed to interlayer water.[28] The onset temperature of QPVP is ∼306 °C. Upon polycation adsorption two thermal regions were observed, at ∼306 °C (exhibiting a broader temperature range), similar to the polycation, and at 480−800 °C. This shift to higher temperature is attributed to polycation thermal stability induced by its intercalation.[28] The latter thermal region also includes mass loss at 604 °C which is assigned to dehydroxylation of the clay.[45]

The mass loss for QPVP 0 M- and QPVP 0.01 M-MMT composites at a high temperature of 739 °C was not observed for the QPVP 1 M-MMT composite. This observation corresponds to an intercalated train configuration of QPVP prepared from a low *IS* solution. For the QPVP 1 M-MMT composite, a shift in mass loss to a lower temperature of 532 °C can be explained by clay exfoliation (Figure 2b). Exfoliation exposes intercalated polycation, thus reducing polycation thermal stability.

DOI: 10.1021/acs.est.6b02167
Environ. Sci. Technol. 2016, 50, 8246−8254

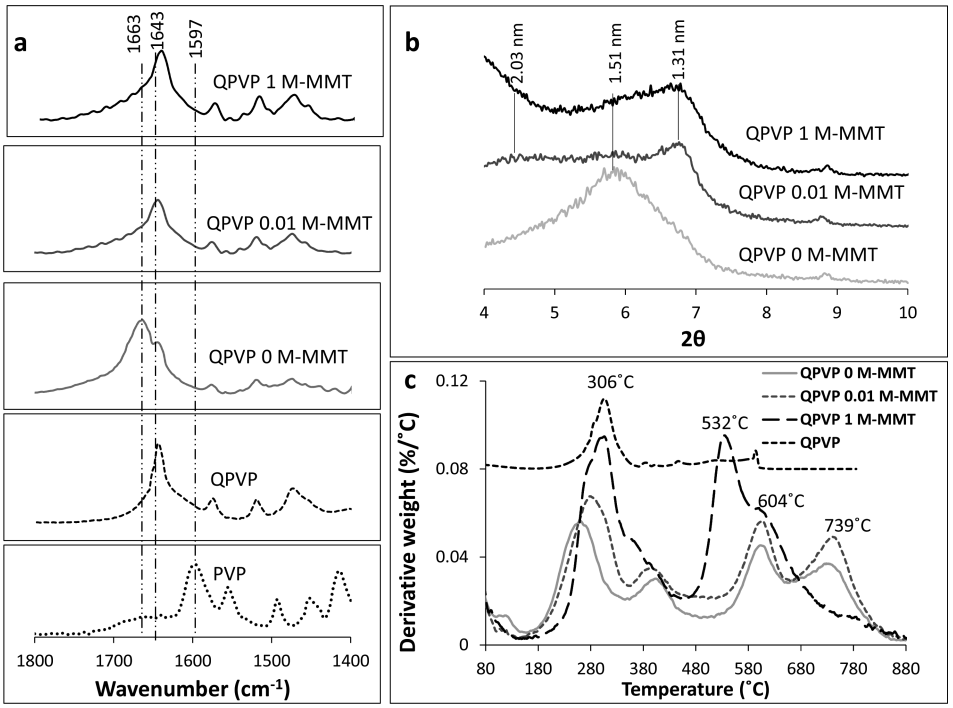

Figure 2. Characterization of QPVP-MMT composites prepared under different *IS*. (a) FTIR spectra (b) XRD diffractograms and (c) DTG analysis profiles.

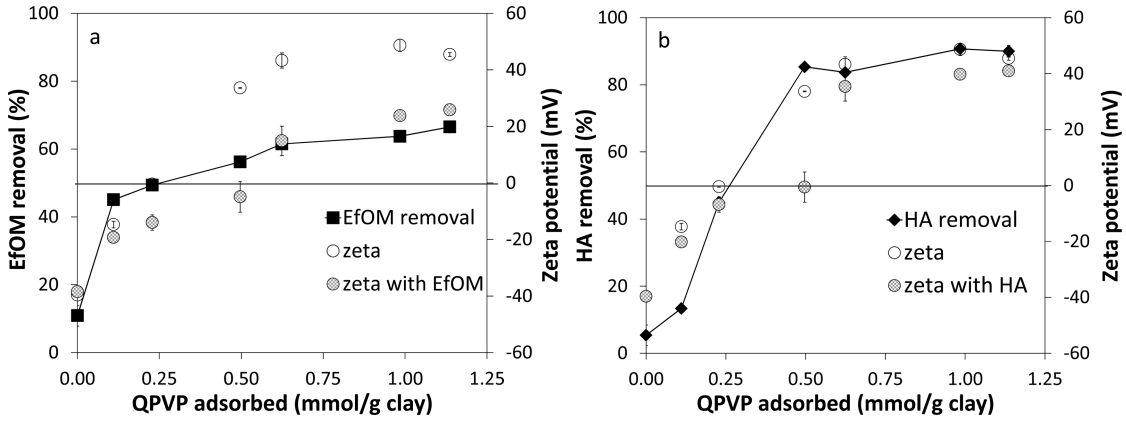

Figure 3. Removal of (a) EfOM (12.2 mg/L DOC) and (b) HA (3 mg/L DOC) by QPVP-MMT composites as a function of QPVP loading and composite zeta potential.

The conclusion that QPVP adsorption to MMT at high *IS* shifts from a flat to a more extended configuration of loops and tails, is in agreement with the litrature.[33,39] This has been shown for the case of polycation adsorption on simple homogeneous surfaces by force field measurements,[46] multi-angled dynamic light scattering,[47,48] NMR solvent relaxation,[49] mean-field theory calculations[50] and Monte Carlo simulations.[51]

The effect of QPVP loading, configuration on the clay (induced by *IS*) and composite zeta potential on EfOM removal efficiency was further explored.

Adsorption of EfOM by Composites. Previous findings indicated that adsorption of HA (zeta potential −39 mV) is governed by a positive zeta potential of the sorbent.[27,52] However, EfOM contains smaller, less charged components as well as highly charged humic substances,[37] and the effect of composite zeta potential on EfOM may be less pronounced and the effect of nonspecific interactions more dominant. To investigate the degree of the effect of composite zeta potential on EfOM adsorption, the adsorption of EfOM by QPVP-MMT composites bearing negative and positive zeta potentials, was investigated (Figure 3). Zeta potentials of QPVP 0 M-, QPVP 0.01 M-, and QPVP 1 M-MMT are highly positive (40−45 mV) therefore composites with QPVP loadings lower than that of QPVP 0 M-MMT (1.1 mmol QPVP/g clay) were studied. Charge neutralization was reached at 0.23 mmol QPVP/g clay, roughly 30% of the cation exchange capacity, due to electrostatic screening of the clay surface (−40 mV) by QPVP (+54 mV).

EfOM removal increased moderately with QPVP loading, from 45 to 49%, which also correlated with less negative values of zeta potential (Figure 3a). EfOM adsorption by positively charged composites further increased to 65%. Upon EfOM adsorption, zeta potential of the composites decreased due to EfOM adsorption and due to electrostatic screening induced by the high electrolyte concentration of the effluent (EC = 1.5 dS/

DOI: 10.1021/acs.est.6b02167
Environ. Sci. Technol. 2016, 50, 8246−8254

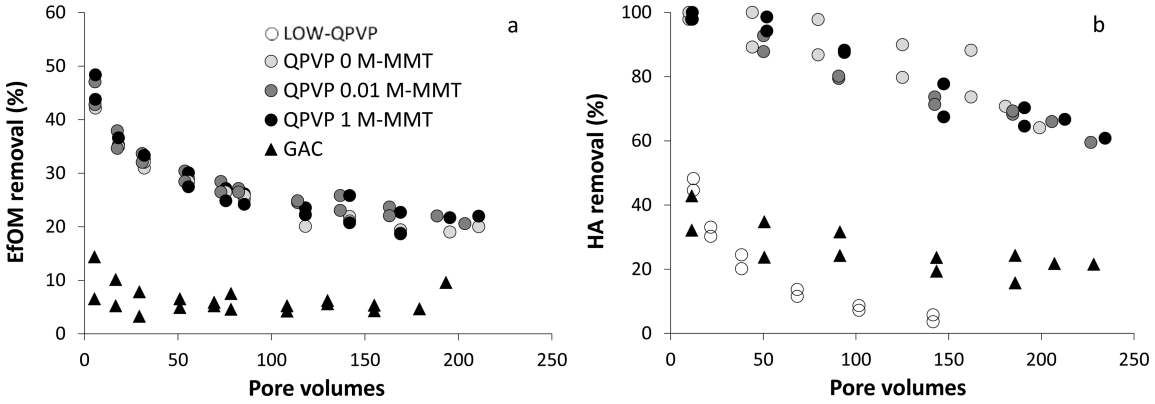

Figure 4. Filtration of (a) EfOM (12.2 mg/L DOC) and (b) HA (3 mg/L DOC) by Low QPVP-, QPVP 0 M-, QPVP 0.01 M- QPVP 1 M-MMT composites, and GAC columns.

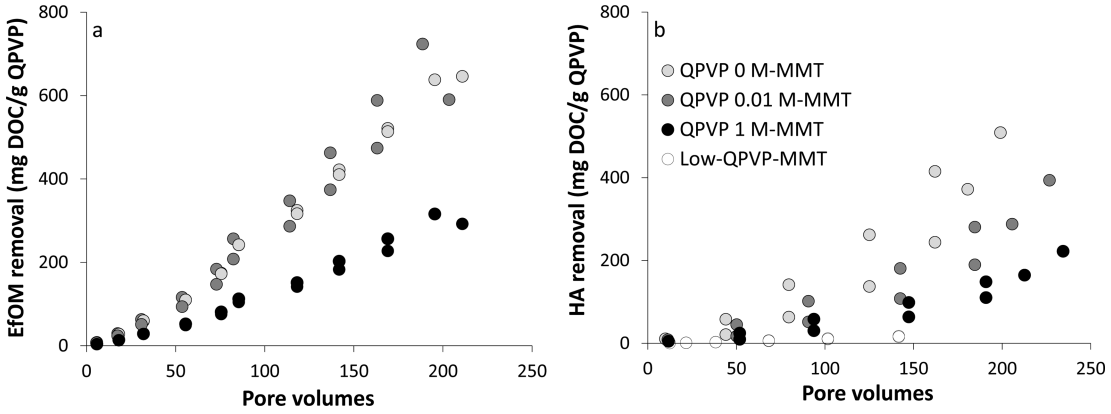

Figure 5. Filtration of (a) EfOM and (b) HA by of QPVP 0 M-, QPVP 0.01 M-, and QPVP 1 M-MMT composite columns normalized to polycation loading (mg DOC/g QPVP).

m). Similar to the previous studies a dominant effect of composite zeta potential was obtained for the removal of HA (95%) (Figure 3b).[27,52] In the case of HA a threshold in zeta potential was observed with an abrupt increase in its removal upon composite charge reversal. The observed differences between EfOM and HA adsorption can then be attributed to their respective properties. EfOM is negatively charged (−21 mV) but contains a large fraction of low molecular weight, low charged compounds,[37,38] which are less prone to electrostatic interactions with positively charged QPVP-MMT composites.[37,52] Indeed, EfOM treatment poses a challenge due to its high heterogeneity and high electrolyte background.

Filtration of EfOM by Composite and GAC Columns. The filtration of EfOM by columns of composites with similar positive zeta potentials (45 mV) but different configurations, QPVP 0 M-, QPVP 0.01 M-, and QPVP 1 M-MMT was studied and compared to the filtration by GAC columns (Figure 4a).

The filtration of EfOM throughout the entire experiment was more efficient (% removal) by QPVP composite columns, approximately 3-fold higher, than by the GAC columns. EfOM may adsorb to both sorbents via nonspecific interactions. The low removal of EfOM by the GAC can be attributed to its negative surface charge (−22 mV) as well as pore clogging.[53,54] On the other hand, the higher removal by the composites can be attributed to electrostatic interaction with the negatively charged components of EfOM, despite the fact that electrostatic interactions are not as dominant as in the case of HA filtration (Figure 4b).

Interestingly, the overall EfOM removal by filtration columns was not affected by QPVP configuration. Moreover, when plotting EfOM or HA removal efficiency normalized to QPVP loading (Figure 5) (since the polycation is the adsorbing component in the composite) it is evident that the removal by the QPVP 1 M composite is the lowest. The cumulative removal (of HA) by the negatively charged composite (Low QPVP-MMT) was the lowest, thus, the negative charge and not the low polycation loading led to low removal (Figure 4b).

Finally, the filtration at a larger scale of EfOM by QPVP 0 M-MMT (which was found more cost-effective than QPVP 1 M-MMT) was compared to the filtration by two different GAC columns and soil from the Shafdan area (Figure 6). EfOM filtration by the composite columns was significantly higher (80 to 60% removal) than by the Shafdan soil (10 to 5% removal) and both GAC columns (70 to 30% removal) throughout the entire experiment.

Effect of Polycation Configuration on Micropollutant Removal. Although it appears that QPVP adsorbed configuration and/or loading did not play a role in overall removal of EfOM, it is reasonable that the higher loading and/or a loops and tails configuration will be beneficial for the removal of anionic micropollutants which are within the size range of QPVP loops and tails. We hypothesized that the removal by QPVP 0.01 M- and QPVP 1 M-MMT would be superior to that of QPVP 0 M−MMT due to the loops and tails

DOI: 10.1021/acs.est.6b02167
Environ. Sci. Technol. 2016, 50, 8246−8254

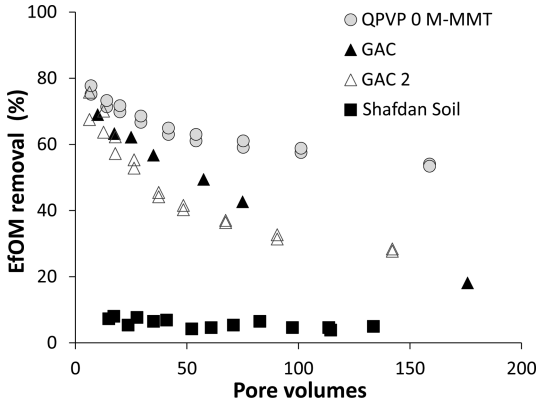

Figure 6. Filtration of EfOM (12.2 mg/L DOC) by columns of QPVP 0 M-MMT composite, two GACs and Shafdan soil.

configuration, resulting in a greater number of QPVP monomers available for adsorption.

To test this hypothesis, we measured the adsorption of three anionic pharmaceuticals: diclofenac (DCF), gemfibrozil (GFZ) and ibuprofen (IBU), from tap water and from Shafdan effluent, to QPVP 0 M-, QPVP 0.01 M-, and QPVP 1 M-MMT. The micropollutants were added at the same organic carbon concentrations as the EfOM (12.2 mg/L DOC), which, although are not environmental concentrations, enabled to study the adsorption mechanism. The interactions between the EfOM and the micropollutants were negligible (see Methods section).

In all cases, micropollutant removal by the composites was in the order of QPVP 0 M-MMT < QPVP 0.01 M-MMT < QPVP 1 M-MMT (Figure 7). Since polymer loading in the QPVP 0 M-MMT and in the QPVP 0.01 M-MMT composites is similar and micropollutant removal was higher by the QPVP 0.01 M-MMT composite, the contribution of this composite's structure as loops and tails, is expressed. Micropollutant removal was highest by the QPVP 1 M-MMT which may be attributed to its high loading. However, when normalizing micropollutant removal to QPVP loading, the removal of GFZ and of IBU from EfOM was higher by QPVP 1 M-MMT, than by QPVP 0 M-MMT (see SI Table S4) supporting the insight that a configuration of loops and tails provides unique binding sites. Due to the extremely high removal of DCF by all three composites (an increase of ~10 and 20% was obtained for the removal by QPVP 0.01 M- and QPVP 1 M-MMT, respectively) the advantage of the loops and tails was not expressed when normalizing to polymer loading (see SI Table S4).

As expected, micropollutant removal from EfOM (EC = 1.5 dS/m) was lower than from tap water (EC = 0.6 dS/m). The degree of reduction varied between the micropollutants, indicating their different interactions with the composites (to be addressed in future studies). The reduction in removal of each micropollutant (represented by values above arrows) by the composites was in the order of QPVP 0 M-MMT > QPVP 0.01 M-MMT > QPVP 1 M-MMT. These results support our hypothesis that a loops a tails configuration offers unique binding sites for micropollutants which are overseen by the bulk EfOM. In addition, these insights may explain our previous observation that the filtration of atrazine and diclofenac (at environmentally relevant concentrations) in the presence of DOM by the GAC columns was reduced, while the removal by composites with loops and tails configuration was not compromised and remained high.[26,28]

We demonstrated that efficient EfOM removal was obtained by employing a QPVP-MMT composite that has a low polycation loading, yet is positively charged. Higher polycation loading, adsorbed as loops and tails, offered unique binding sites for anionic micropollutants which were overseen by the bulk EfOM. Micropollutants may compete for binding sites with other EfOM components but independent binding on unique sites may occur as well. For the removal of nonionic and/or more hydrophobic micropollutants, present in EfOM, further studies will include designing composites with copolymers, of cationic and hydrophobic monomers, in which the cations adsorb to the clay and the loops and tails are hydrophobic domains. This approach of tuning composite properties to bind, with high affinity, different classes of organic pollutants, may enable treating complex water matrixes by employing various composite designs in a filtration system.

■ ASSOCIATED CONTENT

Supporting Information

The Supporting Information is available free of charge on the ACS Publications website at DOI: 10.1021/acs.est.6b02167.

General properties of Shafdan secondary effluent (S1). Correlation between DOC and UV_{254} (S2). QPVP release from filtration columns (S3). Adsorption of pharmaceuticals to QPVP composites (S4) (PDF)

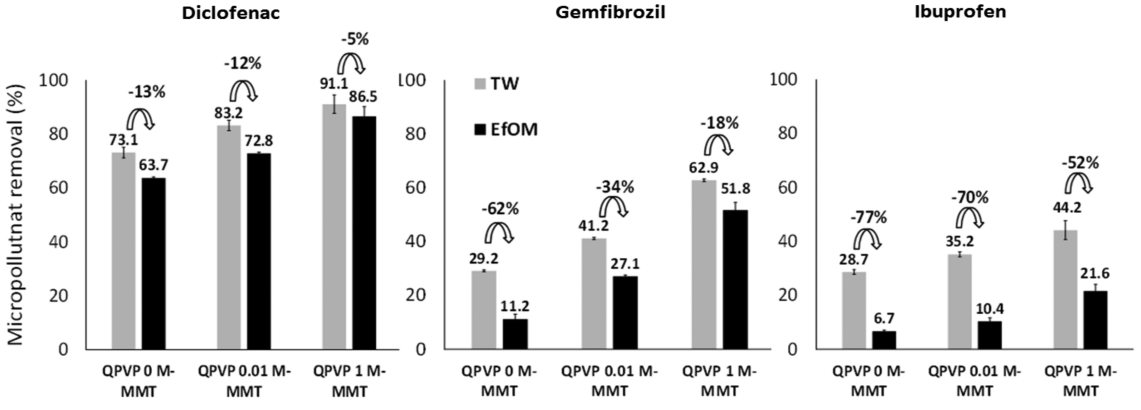

Figure 7. Removal of diclofenac, gemfibrozil and ibuprofen by QPVP 0 M-, QPVP 0.01 M- and QPVP 1 M-MMT composites from tap water (TW) and Shafdan effluent (EfOM). Values above arrows represent decrease in micropollutant removal between TW and EfOM for each composite.

DOI: 10.1021/acs.est.6b02167
Environ. Sci. Technol. 2016, 50, 8246−8254

AUTHOR INFORMATION

Corresponding Author

*Phone: 972-8-948-9171; fax: 972-8-948-9856; e-mail: yael.mishael@mail.huji.ac.il.

Notes

The authors declare no competing financial interest.

ACKNOWLEDGMENTS

This research was supported by the Israeli Ministry of Trade and Industry, Kamin Project (grant 54914) by the Israeli Ministry of Agriculture.

REFERENCES

(1) *Water Reuse: Potential for Expanding the Nation's Water Supply Through Reuse of Municipal Wastewater*; National Research Council: Washington D.C., 2012.

(2) Drewes, J. E.; Quanrud, D. M.; Amy, G. L.; Westerhoff, P. K.; Sites, F. Character of organic matter in soil-aquifer treatment systems. *J. Environ. Eng.* **2006**, *132*, 1447−1458.

(3) Amy, G.; Drewes, J. Soil aquifer treatment (SAT) as a natural and sustainable wastewater reclamation/reuse technology: Fate of wastewater effluent organic matter (EfOM) and trace organic compounds. *Environ. Monit. Assess.* **2007**, *129*, 19−26.

(4) Shon, H. K.; Vigneswaran, S.; Snyder, S. A. Effluent organic matter (EfOM) in wastewater: Constituents, effects, and treatment. *Crit. Rev. Environ. Sci. Technol.* **2006**, *36*, 327−374.

(5) Lindqvist, N.; Tuhkanen, T.; Kronberg, L. Occurrence of acidic pharmaceuticals in raw and treated sewages and in receiving waters. *Water Res.* **2005**, *39*, 2219.

(6) Schwarzenbach, R. P. The Challenge of Micropollutants in Aquatic Systems. *Science (Washington, DC, U. S.)* **2006**, *313*, 1072−1077.

(7) Icekson-Tal, N.; Avraham, O.; Sack, J.; Cikurel, H. Water reuse in Israel − the Dan Region Project: evaluation of water quality and reliability of plant's operation. *Water Supply* **2003**, *3*, 231−237.

(8) Lin, C.; Eshel, G.; Negev, I.; Banin, A. Long-term accumulation and material balance of organic matter in the soil of an effluent infiltration basin. *Geoderma* **2008**, *148*, 35−42.

(9) Lin, C.; Eshel, G.; Negev, I.; Banin, A. Long-term accumulation and material balance of organic matter in the soil of an effluent infiltration basin. *Geoderma* **2008**, *148*, 35−42.

(10) Nadav, I.; Arye, G.; Tarchitzky, J.; Chen, Y. Enhanced infiltration regime for treated-wastewater purification in soil aquifer treatment (SAT). *J. Hydrol.* **2012**, *420−421*, 275−283.

(11) Arye, G.; Tarchitzky, J.; Chen, Y. Treated wastewater effects on water repellency and soil hydraulic properties of soil aquifer treatment infiltration basins. *J. Hydrol.* **2011**, *397*, 136−145.

(12) Oren, O.; Gavrieli, I.; Burg, A.; Guttman, J.; Lazar, B. Manganese mobilization and enrichment during soil aquifer treatment (SAT) of effluents, the Dan Region Sewage Reclamation Project (Shafdan), Israel. *Environ. Sci. Technol.* **2007**, *41*, 766−772.

(13) Rosario-Ortiz, F. L.; Mezyk, S. P.; Doud, D. F. R.; Snyder, S. A. Quantitative correlation of absolute hydroxyl radical rate constants with non-isolated effluent organic matter bulk properties in water. *Environ. Sci. Technol.* **2008**, *42*, 5924−5930.

(14) Jarusutthirak, C.; Amy, G.; Croué, J. P. Fouling characteristics of wastewater effluent organic matter (EfOM) isolates on NF and UF membranes. *Desalination* **2002**, *145*, 247−255.

(15) Zheng, X.; Khan, M. T.; Croue, J. Contribution of effluent organic matter (EfOM) to ultrafiltration (UF) membrane fouling: Isolation, characterization, and fouling effect of EfOM fractions. *Water Res.* **2014**, *65*, 414−424.

(16) Kim, H. C.; Dempsey, B. a. Comparison of two fractionation strategies for characterization of wastewater effluent organic matter and diagnosis of membrane fouling. *Water Res.* **2012**, *46*, 3714−3722.

(17) Krasner, S. W.; Westerhoff, P.; Chen, B.; Rittmann, B. E.; Amy, G. Occurrence of disinfection byproducts in United States wastewater treatment plant effluents. *Environ. Sci. Technol.* **2009**, *43*, 8320−8325.

(18) Zhang, H.; Qu, J.; Liu, H.; Zhao, X. Characterization of isolated fractions of dissolved organic matter from sewage treatment plant and the related disinfection by-products formation potential. *J. Hazard. Mater.* **2009**, *164*, 1433−1438.

(19) Vigneswaran, S.; Shon, H. K.; Kandasamy, J.; Shim, W. G. Performance of granular activated carbon (GAC) adsorption and biofiltration in the treatment of biologically treated sewage effluent. *Sep. Sci. Technol.* **2007**, *42*, 3101−3116.

(20) Qian, F.; Sun, X.; Liu, Y.; Xu, H. Removal and transformation of effluent organic matter (EfOM) in biotreated textile wastewater by GAC/O3 pre-oxidation and enhanced coagulation. *Environ. Technol.* **2012**, *34*, 1513−1520.

(21) Wei, L. L.; Zhao, Q. L.; Xue, S.; Chang, C. C.; Tang, F.; Liang, G. L.; Jia, T. Reduction of trihalomethane precursors of dissolved organic matter in the secondary effluent by advanced treatment processes. *J. Hazard. Mater.* **2009**, *169*, 1012−1021.

(22) Shon, H. K.; Vigneswaran, S.; Kim, I. S.; Cho, J.; Ngo, H. H. The effect of pretreatment to ultrafiltration of biologically treated sewage effluent: a detailed effluent organic matter (EfOM) characterization. *Water Res.* **2004**, *38*, 1933−1939.

(23) Beall, G. The use of organo-clays in water treatment. *Appl. Clay Sci.* **2003**, *24*, 11−20.

(24) Unuabonah, E. I.; Taubert, A. Clay−polymer nanocomposites (CPNs): Adsorbents of the future for water treatment. *Appl. Clay Sci.* **2014**, *99*, 83−92.

(25) Ruiz-Hitzky, E.; Aranda, P.; Darder, M.; Rytwo, G. Hybrid materials based on clays for environmental and biomedical applications. *J. Mater. Chem.* **2010**, *20*, 9306.

(26) Zadaka, D.; Nir, S. Radian, A.; Mishael, Y. G. Atrazine removal from water by polycation-clay composites: effect of dissolved organic matter and comparison to activated carbon. *Water Res.* **2009**, *43*, 677−683.

(27) Radian, A.; Mishael, Y. Effect of humic acid on pyrene removal from water by polycation-clay mineral composites and activated carbon. *Environ. Sci. Technol.* **2012**, *46*, 6228−6235.

(28) Kohay, H.; Izbitski, A.; Mishael, Y. G. Developing Polycation-Clay Sorbents for Efficient Filtration of Diclofenac: Effect of Dissolved Organic Matter and Comparison to Activated Carbon. *Environ. Sci. Technol.* **2015**, *49*, 9280−9288.

(29) Yu, Z.; Peldszus, S.; Huck, P. M. Adsorption of selected pharmaceuticals and an endocrine disrupting compound by granular activated carbon. 1. Adsorption capacity and kinetics. *Environ. Sci. Technol.* **2009**, *43*, 1467−1473.

(30) Corwin, C. J.; Summers, R. S. Scaling trace organic contaminant adsorption capacity by granular activated carbon. *Environ. Sci. Technol.* **2010**, *44*, 5403−5408.

(31) Mishael, Y. G.; Dubin, P. L. Uptake of organic pollutants by silica-polycation-immobilized micelles for groundwater remediation. *Environ. Sci. Technol.* **2005**, *39*, 8475−8480.

(32) Dobrynin, A. V.; Rubinstein, M. Effect of short-range interactions on polyelectrolyte adsorption at charged surfaces. *J. Phys. Chem. B* **2003**, *107*, 8260−8269.

(33) Xie, F.; Nylander, T.; Piculell, L.; Utsel, S.; Wågberg, L.; Åkesson, T.; Forsman, J. Polyelectrolyte adsorption on solid surfaces: theoretical predictions and experimental measurements. *Langmuir* **2013**, *29*, 12421−12431.

(34) Van de Steeg, H. G. M.; Cohen Stuart, M. a.; De Keizer, A.; Bijsterbosch, B. H. Polyelectrolyte adsorption: a subtle balance of forces. *Langmuir* **1992**, *8*, 2538−2546.

(35) Kam, S. K.; Gregory, J. The interaction of humic substances with cationic polyelectrolytes. *Water Res.* **2001**, *35*, 3557−3566.

(36) *Standard Methods for the Examination of Water and Wastewater*, 19th ed.; Eaton, A. D., Clesceri, L. S., G, A., Ed.; American Public Health Association: Washington D.C., 1995.

DOI: 10.1021/acs.est.6b02167
Environ. Sci. Technol. 2016, 50, 8246−8254

(37) Kim, H. C.; Dempsey, B. A. Membrane fouling due to alginate, SMP, EfOM, humic acid, and NOM. *J. Membr. Sci.* **2013**, *428*, 190−197.
(38) Goren, U.; Aharoni, A.; Kummel, M.; Messalem, R.; Mukmenev, I.; Brenner, A.; Gitis, V. Role of membrane pore size in tertiary flocculation/adsorption/ultrafiltration treatment of municipal wastewater. *Sep. Purif. Technol.* **2008**, *61*, 193−203.
(39) Sukhishvili, S. A.; Granick, S. Polyelectrolyte adsorption onto an initially-bare solid surface of opposite electrical charge. *J. Chem. Phys.* **1998**, *109*, 6861.
(40) Liufu, S. C.; Xiao, H. N.; Li, Y. P. Adsorption of cationic polyelectrolyte at the solid/liquid interface and dispersion of nanosized silica in water. *J. Colloid Interface Sci.* **2005**, *285*, 33−40.
(41) Durand, G.; Lafuma, F.; Audebert, R. Adsorption of cationic polyelectrolytes at clay-colloid interface in dilute aqueous suspensions — effect of the ionic strength of the medium. In *Trends in Colloid and Interface Science II SE- 47*; Degiorgio, V., Ed.; Progress in Colloid & Polymer Science; Steinkopff, 1988; Vol. *76*, pp 278−282.
(42) Smith, P.; Eisenberg, A. Infrared spectroscopic study of blends of poly (styrene-co-styrenesulfonic acid) with poly (styrene-co-(4-vinylpyridine)). *Macromolecules* **1994**, *27*, 545−552.
(43) Khaligh, N. G.; Shirini, F. Preparation, characterization and use of poly(4-vinylpyridinium) hydrogen sulfate salt as an eco-benign, efficient and reusable solid acid catalyst for the chemoselective 1,1-diacetate protection and deprotection of aldehydes. *J. Mol. Catal. A: Chem.* **2011**, *348*, 20−29.
(44) Fournaris, K. G.; Karakassides, M. A.; Petridis, D.; Yiannakopoulou, K. Clay-polyvinylpyridine nanocomposites. *Chem. Mater.* **1999**, *11*, 2372−2381.
(45) Guggenheim, S.; Groos, A. F. K. van. Baseline studies of the clay minerals society of source clay minerals: Thermal analysis. *Clays Clay Miner.* **2001**, *49*, 433−443.
(46) Marra, J.; Hair, M. L. Forces between two poly (2-vinylpyridine)-covered surfaces as a function of ionic strength and polymer charge. *J. Phys. Chem.* **1988**, *92*, 6044−6051.
(47) Seyrek, E.; Hierrezuelo, J.; Sadeghpour, A.; Szilagyi, I.; Borkovec, M. Molecular mass dependence of adsorbed amount and hydrodynamic thickness of polyelectrolyte layers. *Phys. Chem. Chem. Phys.* **2011**, *13*, 12716−12719.
(48) Hierrezuelo, J.; Szilagyi, I.; Vaccaro, A.; Borkovec, M. Probing nanometer-thick polyelectrolyte layers adsorbed on oppositely charged particles by dynamic light scattering. *Macromolecules* **2010**, *43*, 9108−9116.
(49) Nelson, A.; Jack, K. S.; Cosgrove, T.; Kozak, D. NMR solvent relaxation in studies of multicomponent polymer adsorption. *Langmuir* **2002**, *18*, 2750−2755.
(50) Shafir, A.; Andelman, D.; Netz, R. Adsorption and depletion of polyelectrolytes from charged surfaces. *J. Chem. Phys.* **2003**, *19*, 2355−2362.
(51) Beltran, S.; Harvey, H. H.; Prausnitz, J. M. Monte Carlo study of polyelectrolyte adsorption. Isolated chains on a planar charged surface. *Macromolecules* **1991**, *24*, 3178−3184.
(52) Zhang, X.; Bai, R. Mechanisms and kinetics of humic acid adsorption onto chitosan-coated granules. *J. Colloid Interface Sci.* **2003**, *264*, 30−38.
(53) Quinlivan, P. A.; Li, L.; Knappe, D. R. U. Effects of activated carbon characteristics on the simultaneous adsorption of aqueous organic micropollutants and natural organic matter. *Water Res.* **2005**, *39*, 1663−1673.
(54) Pelekani, C.; Snoeyink, V. L. Competitive adsorption between atrazine and methylene blue on activated carbon: the importance of pore size distribution. *Carbon* **2000**, *38*, 1423−1436.

DOI: 10.1021/acs.est.6b02167
Environ. Sci. Technol. 2016, 50, 8246−8254